Available online at www.sciencedirect.com

ScienceDirect

IFAC Papers Online CONFERENCE PAPER ARCHIVE

IFAC PapersOnLine 51-28 (2018) 616–621

Deep Flux-Weakening Strategy with MTPV for High-Speed IPMSM for Vehicle Application

Maurice Fadel, Leopold Sepulchre, Maria Pietrzak-David

LAPLACE, Université de Toulouse, CNRS INPT, UPS, 2 rue Charles Camichel, F-31071 Toulouse, France.

Abstract: High speed Interior Permanent Magnet Synchronous Motors (IPMSM) are used in embedded applications for their high-power density and efficiency. Because of the voltage limit of the supply, operating at such speed requires to do flux-weakening by adding negative Id current. The optimal current reference trajectory in the d-q frame for a torque reference that minimized the current norm while respecting the current and voltage limits, is calculated. When all the magnet contribution to the airgap is compensated, the trajectory that maximizes the power output is the Maximum Torque Per Volt (MTPV) trajectory and this one doesn't correspond to maximum current operation. In this paper is proposed a new flux-weakening algorithm that includes the MTPV trajectory without algorithm switching. A second variable current limit is added that corresponds to the current norm required by the analytical MTPV solution. A description of the existing deep-flux-weakening techniques is carried out. The efficiency of the proposed method is validated and compared to existing techniques throw experiments on a small scaled motor. The results show an increase of the torque (and power) and a reduction of the losses when operating at very high speed. Finally, an over speed of 9,23 is reached.

Keywords: PMSM – High Speed – Flux Weakening – Maximum Torque Per Volt.

1. INTRODUCTION

The torque/speed characteristic of a PMSM for vehicle application presents a maximal constant torque at low speed, and a wide speed range at constant power. Its maximal torque determines the size and mass of a PMSM. It is possible to make a PMSM with less maximal torque, the same power and that is able to operate at higher rotational speed. The desired torque/speed characteristic for the car is then retrieved by adapting the output gear. The high speed PMSM obtained is smaller and lighter than the traditional one while having the same power that makes it and advantage for transport application. This work is part of the study on how to drive such a PMSM.

Flux-weakening techniques have been the subject of many publications in recent years. We propose to classify these strategies in the following way:

-Algorithm by direct analytical calculation [7]. The authors analytically compute the current references for a smooth-pole MSAP and a salient-pole MSAP with analytical switching of algorithms between the trajectories. However, they do not take into account the MTPV trajectory.

-With LUT (Look Up Tables) and torque and flux considerations like TFC algorithm (Torque and Flux Control). [13]. However, this approach is motor-dependent and requires a set of experiments to be performed beforehand (and therefore longer to implement than other commands), or to generate the LUTs with a fine-element approach. The outputs of the LUTs are torque and flux references, which can be directly used by a Direct Torque Control method or converted to current.

-With a single regulator for the current loop: SCR (Single Current Regulator) [9] - [12]. The SCR control makes it easy to take into account the voltage saturation by current loop. The corrector acts on the angle of the voltage vector whose norm is fixed at the maximum voltage. The SCR method exhibits low stability and high sensitivity to the regulator parameters. In addition, the current limit is not considered because only the current of the d-axis is controlled. Finally, the SCR requires switching to another control algorithm when the PMSM is not running in voltage saturation.

-With vector control and regulation on the voltage norm or with modification of the angle of the current vector or with modification of the current value Id.

This article presents a flux-weakening strategy that takes into account the MTPV trajectory, and in a unified way. First the desired optimal d-q current references are calculated analytically and the achievable operating points regarding the electrical limits are shown. Secondly a review of the existing flux-weakening techniques is done. A special focus is made on the strategies that include the MTPV trajectory. Thirdly the proposed deep flux-weakening strategy is presented. Finally, experimental results on a scaled motor are shown. They validate that the control algorithm proposed is able to drive the PMSM at a very high over-speed coefficient i.e. usually twice the nominal speed, here it reaches more than 9 times that speed. The experimental results are compared to those obtained with common flux-weakening strategies. A proposed solution is to use a hybrid algorithm with this direct feedforward computation associated with an online-tracking algorithm to optimize the value of the current references.

10.1016/j.ifacol.2018.11.772

2. OPTIMAL DESIRED ID IQ CURRENT REFERENCES

2.1 PMSM model

The electrical model of the PSMS in the rotor rotating d-q frame with the convention of the conservation of electrical quantities can be expressed as (1) and (2). The torque expression is given by (3).

$$V_d = R.I_d + L_d \frac{dI_d}{dt} - \omega.L_q.I_q \quad (1)$$

$$V_q = R.I_q + L_q \frac{dI_q}{dt} + \omega.L_q.I_q + \omega.\phi_f \quad (2)$$

$$T = \frac{3}{2}.p.\left(\phi_f.I_q + (L_d - L_q)I_d I_q\right) \quad (3)$$

Where V_d, V_q, I_d and I_q are respectively the voltage and the current in the d-q frame, ω is the electrical rotor angle velocity, T is the electromagnetic torque, and the other parameters are described in Table 1.

The current limit I_{max} (4) takes into account the cooling limits of the PMSM and the inverter, and the maximum current that can deliver the battery (brought back on an equivalent motor current).

$$\sqrt{\left(I_d^2 + I_q^2\right)} \le I_{\max} \quad (4)$$

The voltage limit (5) depends on the battery voltage V_{DC} and the PWM strategy used, here a SVPWM.

$$\sqrt{\left(V_d^2 + V_q^2\right)} \le V_{\max} \quad \text{and} \quad V_{\max} = \frac{V_{DC}}{\sqrt{3}} \quad (5)$$

At high speed the voltage drop associated with the resistance R is usually negligible compared to the *e.m.f* (electromotive force), and (5) can be rewritten with (1) and (2) as (6).

$$\sqrt{\left(\omega.L_q.I_q\right)^2 + \left(\omega.L_d.I_d + \omega.\phi_f\right)^2} \le V_{\max} \quad (6)$$

The critical point $I_{critical}$ (7) is defined as the center of the ellipse of the voltage limit (6). It corresponds to the d axis current reference point achieving a total flux-weakening compensation of the magnet contribution to the air gap flux, with zero current on the q-axis, that is to say with a torque also equal to zero.

$$I_{critical} = \left(-\frac{\phi_f}{L_d}\right) \quad (7)$$

2.2 Optimal current references trajectory in d-q frame

The problem can be expressed the following way. The optimal d-q current references are calculated in order to generate the reference torque while respecting the current and the voltage limit and with minimum electrical losses. The minimum loses is approximated by minimizing the current norm. It is a standard approach in PMSM control. [13] compares 4 different strategies: MTPA (Maximum Torque Per Ampere), ME (Maximum Efficiency), MCPT (Minimum Current Point Tracking), and MLPT (Minimum Loss Point Tracking) and concludes that in real time application MTPA should be the predilection choice. Further discussion can be found in [7]. The analytical solution to this problem is plotted in red on Figure 1 in the I_d-I_q frame, for a speed from 0 rpm to 30 krpm and with an initial reference torque of 120 N.m (a little less than the maximum torque 136 N.m in order to illustrate better the different operating areas). On Figure 1 is also plotted the current limit (in blue) (4) that is a circle centred on the origin of the frame and of radius I_{max}. The voltage limit (in green) is an ellipse (6), centered on the critical point (7) which size decrease with the increase of the speed. The dotted curves on Figure 1 are constant torque curves they are calculated from 10 N.m to 150 N.m with a pitch of 10 N.m. They are curved because of the saliency, here L_d is smaller than L_q so adding negative current I_d generates torque if current I_q is non-zero (3).

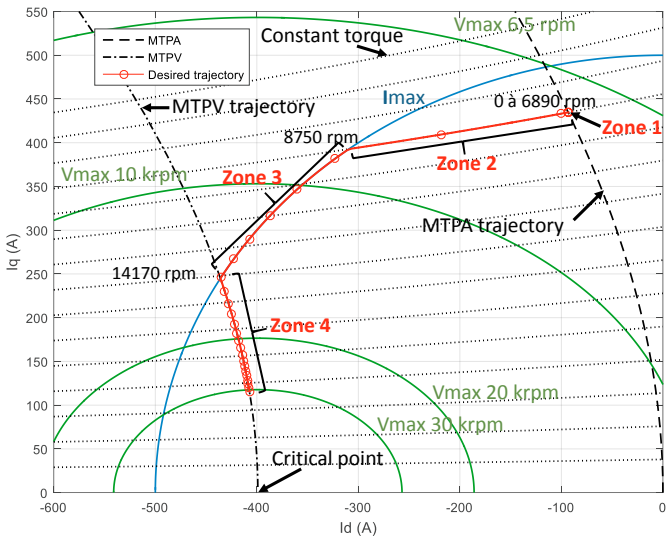

Fig. 1. Representation in the I_d-I_q frame the current limit (blue), the voltage limit (green) for the following speeds 6.5 rpm, 10 krpm, 20 krpm, 30 krpm, and the path travelled by the current references when the speed increases for a torque reference of 120 N.m (red, and red circles every 1000 rpm.)

It is observed that the trajectory of the currents runs 4 zones of operation with the increase of the speed.

In Zone 1 the PMSM operates out of voltage and current limits. The MTPA strategy is used and the problem then formulates as (8). By Lagrange multiplier resolution method, it gives the following results (9) and (10) that are plotted on Figure 1 in dash line. Note that for a smooth pole PMSM the classic I_d equal to 0 strategy would be used.

$$I_d, I_q \Rightarrow \max\ T \quad \text{with} \sqrt{I_d^2 + I_q^2} = I_{norm} \quad (8)$$

Where I_{nom} is the total current norm.

$$I_d = \frac{\phi_f - \sqrt{\phi_f^2 + 8(L_d - L_q)^2 I_{norm}^2}}{-4(L_d - L_q)} \quad (9)$$

$$I_q = \sqrt{I_{norm}^2 - I_d^2} \tag{10}$$

When the speed increases the voltage saturation (6) tightens towards the critical point in the I_d-I_q frame. The PMSM operates on the voltage limit. A first flux-weakening is carried-out following a constant torque curve named Zone 2, equal to the reference torque. The problem is expressed as (3) and (6) with a strict equality. By expressing I_q using (10) then injecting it in (3) squared, we obtain **Erreur ! Source du renvoi introuvable.** that is written as a polynomial of the variable I_d. The I_d current reference can be calculated by solving numerically **Erreur ! Source du renvoi introuvable.** and the I_q reference is then deduced from (10).

$$\begin{aligned} &I_d^4(-(L_d-L_q)^2.L_d^2.\omega^2) \\ &+I_d^3(-2.\phi_f.L_d^2.\omega^2.(L_d-L_q)-2.L_d.\omega^2.\phi_f.(L_d-L_q)^2) \\ &+I_d^2.(-L_d^2.\omega^2.\phi_f^2+(L_d-L_q)^2.(V_{\max}^2-\omega^2.\phi_f^2)) \\ &+I_d.(-2.L_d.\omega^2.\phi_f^3+2.\phi_f.(L_d-L_q).(V_{\max}^2-\omega^2.\phi_f^2)) \\ &+(V_{\max}^2-\omega^2.\phi_f^2).\phi_f^2-\frac{4.T_{ref}^2.L_q^2.\omega^2}{9.p^2}=0 \end{aligned} \tag{11}$$

The torque is maintained while the speed increases until the negative current I_d added makes the current norm reach the current saturation. From this point the PMSM operates on the intersection of the current saturation and the voltage saturation, named Zone 3. The problem is expressed by the equations (4) with exact equalities. The I_d solution is (12) for a salient poles PMSM and the I_q is also deduced from (10).

$$I_d = \frac{L_d\phi_f}{L_d^2-L_q^2} + \frac{\sqrt{L_d^2\phi_f^2-(L_d^2-L_q^2)(\phi_f^2+L_q^2I_{\max}^2-\frac{V_{\max}^2}{\omega^2})}}{L_d^2-L_q^2} \tag{12}$$

For a smooth poles PMSM I_d is given (13).

$$I_d = \frac{V_{\max}^2-\omega^2.\phi_f^2-L_q^2.\omega^2.I_{\max}^2}{2.L_d.\omega^2.\phi_f} \tag{13}$$

If the critical point is outside the current saturation circle then when the speed increases the current references point follows this path (zone 3) until the generated torque vanishes. From this velocity (theoretical in motor mode because the torque is zero), there is no longer any intersection between the space of the points of the permissible operations which respect the saturation of voltage (6) and that which respects the current saturation (4). In other words, if the critical point is greater than the current limit then the problem given by equations (6) and (4) does not admit any more solution. In this case, the speed of the machine is limited electrically.

If the critical point is within the current saturation then this implies that it is possible to generate a flux whose component on the d axis completely compensates for the contribution of the magnet to the flux of the air gap. When current I_d is added

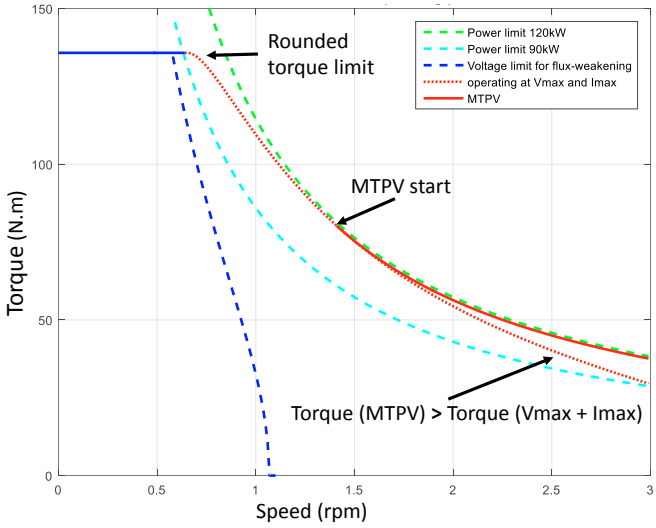

Fig. 2. Limits of the achievable operating points in the torque-speed frame.

for flux-weakening, a moment occurs when all the flux of the magnet is compensated and it is no longer necessary to add negative current I_d to respect the voltage limit. Thus, from that moment, the trajectory MTPV (Maximum Torque Per Volt) is followed. The problem is expressed by (14), obtained with (1), (2) and (3) and by neglecting the voltage drop due to the resistance because of the high rotational speed operation.

$$V_d, V_q \Rightarrow \max T = \frac{3}{2}p\left(\Phi_f+\left(L_d-L_q\right)\left(\frac{V_q}{\omega L_d}-\frac{\Phi_f}{L_d}\right)\right)\left(-\frac{V_d}{\omega L_q}\right) \tag{14}$$
$$\text{with } V_d^2+V_q^2=V_{max}^2$$

By using Lagrange multiplier, we obtain the voltage vector maximizing the torque (15) and (16) giving the current references I_d and I_q by (17).

$$V_q = \frac{\phi_f - \sqrt{\phi_f^{\,2}+V_{\max}^2 8\left(\frac{L_d-L_q}{L_q\omega}\right)^2}}{-4\left(\frac{L_d-L_q}{L_q\omega}\right)} \tag{15}$$

$$V_d = -\sqrt{V_{\max}^2-V_q^2} \tag{16}$$

$$I_d = \frac{\left(\frac{V_q}{\omega}-\phi_f\right)}{L_d} \quad \text{and} \quad I_q = -\frac{V_d}{L_q\omega} \tag{17}$$

For a smooth pole PMSM the current reference are (18).

$$I_d = -\frac{\phi_f}{L_d} \quad \text{and} \quad I_q = \frac{V_{\max}}{L_q.\omega} \tag{18}$$

This strategy makes it possible to generate the torque closest to the reference torque while respecting the voltage and current limits. When the velocity tends towards the infinite this trajectory tends towards the critical point and remains

contained within the electric limits and thus the velocity is not theoretically limited by these saturations. The MTPV trajectory in the I_d-I_q frame is plotted on Figure 1.

With a salient poles PMSM this optimal path allows to flux-weaken beyond the critical point because the current I_d generates torque and using the minimum current norm is a criteria. Here, whatever the velocity there is positive torque which tends to 0 when the speed increases.

Note on demagnetization risks in operation of deep flux weakening. This risk is detailed in [14] and more specifically for MPTV operation in [15]. Demagnetization occurs if the inverse field applied to the magnet exceeds its coercive field which varies with temperature. This risk occurs mainly when the PMSM operates at high temperature and deep flux-weakening, which makes it thus one of the dimensioning elements for the cooling system. The risks of demagnetization are also avoided by the structure of the machine which impacts the field lines through which the flux backs up. Finally, the use of the MTPV strategy induces less risk of demagnetization at high speed than the usual algorithms which do not take this path into account and which flux-weaken more importantly while remaining in zone 3 on the current limit.

In this paper is proposed a flux-weakening algorithm that follows that optimal trajectory for the current references when the speed increases (Zones 1 to 4).

2.3 Achievable operating points

The Figure 2 shows the achievable operating points in the torque-speed frame by plotting the electrical limits. The current limit is a maximum torque limit plotted in solid-blue. The dotted blue line is the torque limit representing the voltage limit when no flux-weakening is performed. The red dotted line is the maximum torque achievable when the PMSM operates in voltage and current saturation (Zone 3). The solid-red line is the torque limit when operating on the MTPV trajectory. The torque generated is above the torque obtained is the references stay in Zone 3 when the speed increase. So at high speed, operating at maximum current and maximum voltage does not give the maximum power!

Thus following the MTPV trajectory enables high speed to generate more torque with a smaller current norm (and thus fewer losses) than if the reference current point continued to follow the intersection between the current and voltage limits (Zone 3). It is the optimum solution that maximizes torque by minimizing the required current standard and respecting current and voltage limits. In the literature (see section 3), the MTPV strategy is rarely included in the control and this one gives references that remain on Zone 3 when the speed is increases. Existing flux-weakening techniques, and the ones that take into account the high-speed MTPV strategy, are presented in section 3. In Section 4 is proposed a control strategy that includes the MTPV trajectory in a unified way.

The green and cyan dotted line are examples of power limit (resp. 120 kW and 90 kW). Usually in the industry we talk about constant torque limit and power limit. However, one can see that the achievable operating points are not exactly a power limit especially when entering in Zone 3. This is considered in the control in addition to the power battery limit.

Table 1. Parameters of PMSM

PMSM mechanical parameters			
J	Inertia	0.13	kg.m^2
f_0	Viscous friction	0.0019	kg.m^2
N_{max}	Maximal rotation speed	30000	rpm
PMSM electrical parameters			
p	Number of pole pairs	2	-
R	Resistance of a phase	6.90	mΩ
L_d	Equivalent inductance on the d axis	220.0	µH
L_q	Equivalent inductance on the q axis	265.4	µH
Φ_f	Magnet Flux perceived by the stator	87.78	mWb
I_{max}	Maximal current (thermal limitation in steady state)	500	A
T_{max}	Torque limit	136	N.m
P_{max}	Power limit estimation	100	kW
Battery parameters			
V_{DC}	DC bus voltage	340	V
Inverter parameters			
f_{dec}	Switching frequency	8	kHz

For confidential reasons, these parameters are not exactly those of the real motor for the vehicle application, but they are representative of an electrical traction application and are used for the simulations in this paper.

3. PROPOSED DEEP FLUX WEAKENING STRATEGY

Figure 3 shows an algorithm for calculating current references when the input is a torque reference given by the user, which is generally the case for automotive applications.

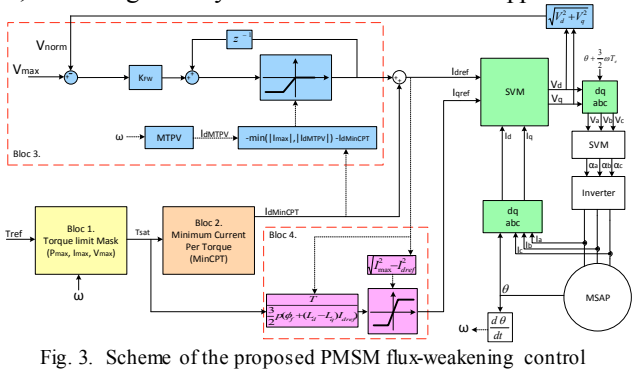

Fig. 3. Scheme of the proposed PMSM flux-weakening control

The flux-weakening control law presented in the diagram, in bloc 3 on Figure 3, here is an integration gain, noted K_{FW}. This structure is sufficient to impose the desired dynamic in a closed loop, and it simplifies the formulation of the corrector and the consideration of the variable saturation by the integration (anti-windup solution). The flux-weakening corrector is thus calculated to impose the desired bandwidth in closed loop from an approximation at the first-order of the current loop whose dynamics is negligible (superior to 100 Hz), in comparison the flux reduction loop bandwidth is set at 10Hz. The bloc 1 on Figure 3 is a saturation of the torque

reference to the theoretically achievable operating points depending on the speed (see Figure 2).

The bloc 2 gives the I_d current reference that minimizes the current norm to achieve the required in entrance. A Minimum Current Per Torque (MinCPT) strategy is used. The problem can be expressed as (19).

$$I_d, I_q \Rightarrow \min(I_d^2 + I_q^2) \quad \text{with } T = \frac{3}{2}.p.\left(\phi_f.I_q + (L_d - L_q)I_d I_q\right) \qquad (19)$$

The current I_d is solution of (20). To facilitate the real-time resolution, a solution, giving I_d depending on the reference torque, and that is numerical of the parameters and analytical from the torque is precalculated.

$$I_d^4.(L_d - L_q)^3 + I_d^3.(L_d - L_q)^2.3.\phi_f + I_d^2.3.\phi_f^2.(L_d - L_q) + I_d \qquad (20)$$

The bloc 4 is used to deduce the Iq current reference form the saturated torque reference and the Id current form the flux weakening plus the MinCPT strategy.

This algorithm allow to follow the optimal trajectory desired (Figure 1) when the speed increases without algorithm commutations.

4. EXPERIMENTAL RESULTS

An experimental setup (Fig. 4) is created in order to validate the relevance of the control laws presented. The objective is to validate that these laws enable to drive the high-speed PMSM and increase the maximum achievable speed, torque and high-speed efficiency as compared to conventional control strategies.

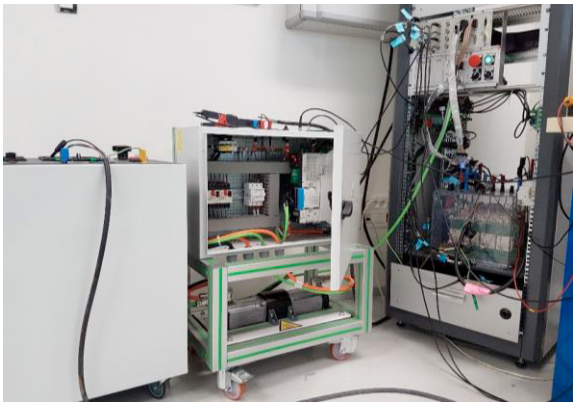

Fig. 4. Experimental Setup

The test-bench uses a reduced power motor whose parameters are shown in Table 2. The torque-speed profile remains that of an electric traction application and the experimental conditions presented in this chapter are representative of a high-speed operation enabling the validation of the control algorithms.

The machine is a smooth poles PMSM is powered through a 3-legs 2-levels inverter and driven by an SVM with at a switching frequency of 8kHz. The control is realized under DSPACE (DS1104) and is the one of Figure 5 with a torque reference. A second identical motor is coupled in opposite direction and operates as a generator connected to a variable speed drive debiting on a resistive load. It imposes a resistive torque and limits the speed to the desired operating point.

Table 2. Parameters of the experimental setup

PMSM mechanical parameters			
J_{total}	Total inertia motor + charge	$2{,}1.10^{-4}$	kg.m²
f_0	Viscous friction	$1{,}8.10^{-4}$	kg.m²
PMSM electrical parameters			
p	Number of pole pairs	5	-
R	Resistance of a phase	1,35	Ω
L_d	Equivalent inductance on the d axis	5,65	µH
L_q	Equivalent inductance on the q axis	5,65	µH
Φ_f	Magnet Flux perceived by the stator	0,0345	Wb
I_{max}	Maximal current (thermal limitation in steady state)	6,20	A
$I_{critical}$	Critical point ($-\Phi_f/L_d$)	-6,10	A
Battery parameters			
V_{DC}	DC bus voltage	50	V
Inverter parameters			
f_{dec}	Switching frequency	8	kHz

Three control algorithms are tested:

- The control algorithm without flux-weakening with the current loop alone. Current references are directly defined by the MinCPT strategy, figure 5.

- The control algorithm with conventional flux-weakening strategy, figure 6.

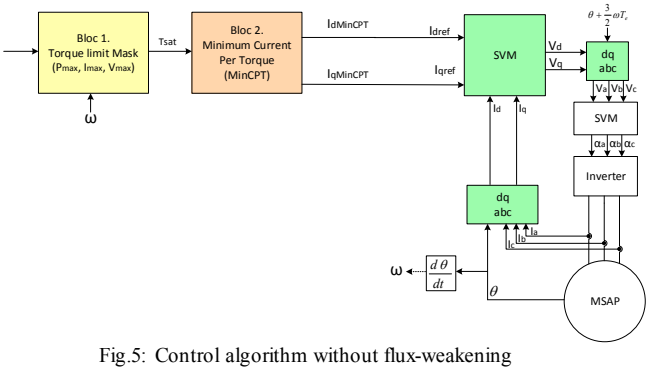

Fig.5: Control algorithm without flux-weakening

- The control algorithm proposed in this paper with the flux-weakening strategy including the MTPV strategy in a unified way (Figure 3).

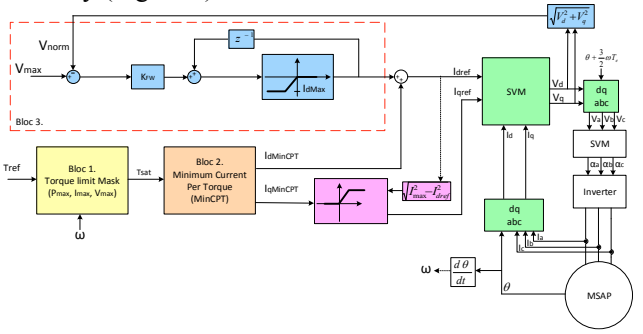

Fig.6: Control algorithm with conventional flux-weakening strategy

As mentioned in the introduction, the three algorithms include the prediction of the variation of the angle (due to the

computation delay and the discontinuous nature of the inverter) for inverse Park transformation [7], [8]. The tests are carried out with a DC bus voltage of 50V. With this voltage and maximum torque set point the flux-weakening starts from 869 rpm. The current limit is 6.20 A. This limit is placed voluntarily a little beyond the critical current of -6.10 A on the d-axis required to completely compensate the magnet contribution to the airgap flux.

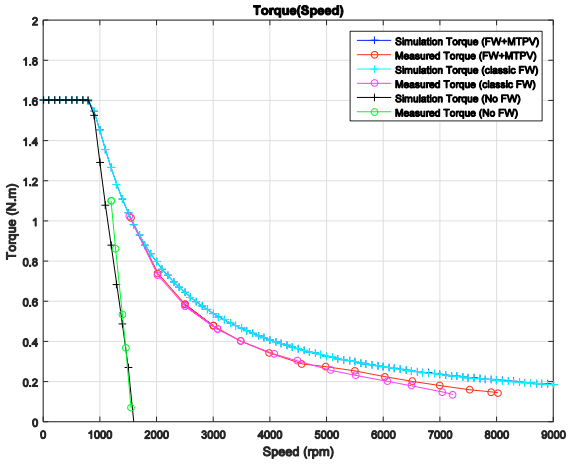

Fig. 7. Torque Speed results in steady state for 3 control strategies.

On Figure 7. Is plotted the torque measured in steady state every 500 rpm. Without flux weakening the maximum speed reached is 1551 rpm, with a classic algorithm it is 7227 rpm and with the algorithm with MTPV 8023 rpm are obtained. These results show the importance of using a flux-weakening algorithm for high-speed operation. More importantly, it also shows that following the MTPV trajectory at high speed enable the PMSM to generate more torque than the classic algorithm that stays on Zone 3, from 5000 rpm to higher speeds. The Figure 7 also illustrates that the proposed algorithm is able to drive the PMSM to a over speed coefficient of 9,23!

5. CONCLUSION

The analytical calculation of the optimal trajectory of the current references depending on the speed for a IPMSM is performed. This trajectory is divided in 4 zones: the MTPA (or MinCPT) at low speed then the references goes throw 3 flux-weakening stages. At high speed the maximum power is given when operating at maximum voltage but not at maximum current; the corresponding trajectory is named MTPV. If the critical point is lower than the maximum current in absolute value, then current references exists theoretically whatever the speed that respect the electrical limits and the MPTV trajectory is the solution at high speed.

In the literature, most flux-weakening strategies don't consider the MTPV strategy and not in a unified way. In this paper is proposed a flux-wakening strategy that takes into account the MTPV Zone of operation by adding a variable virtual current saturation corresponding to the MTPV analytical current norm.

The efficiency of the proposed flux-weakening strategy is validated experimentally on a small scaled motor. The PMSM is able to operate in the 4 zones of operation and reaches a over speed of 9,23. Compared to the classic control strategy, at high speed, the torque is increased and the losses are reduced! This result is interesting for embedded applications such as electrical traction in automobile.

REFERENCES

[1] T. Finken, M. Felden, et K. Hameyer, « Comparison and design of different electrical machine types regarding their applicability in hybrid electrical vehicles », in *Electrical Machines, 2008. ICEM 2008. 18th International Conference on*, 2008, p. 1–5.

[2] J. Driesen et R. Belmans, « Specific problems of high-speed electrical drives », *Micro Gas Turbines*, p. 12–1, 2005.

[3] D. Gerada, A. Mebarki, N. L. Brown, C. Gerada, A. Cavagnino, et A. Boglietti, « High-speed electrical machines: Technologies, trends, and developments », *IEEE Trans. Ind. Electron.*, vol. 61, nº 6, p. 2946–2959, 2014.

[4] A. Borisavljevic, *Limits, modeling and design of high-speed permanent magnet machines*. Springer Science & Business Media, 2012.

[5] P. Cortes, M. P. Kazmierkowski, R. M. Kennel, D. E. Quevedo, et J. Rodriguez, « Predictive Control in Power Electronics and Drives », *IEEE Trans. Ind. Electron.*, vol. 55, nº 12, p. 4312-4324, déc. 2008

[6] F. Morel, X. Lin-Shi, J. M. Retif, B. Allard, et C. Buttay, « A Comparative Study of Predictive Current Control Schemes for a Permanent-Magnet Synchronous Machine Drive », *IEEE Trans. Ind. Electron.*, vol. 56, nº 7, p. 2715-2728, juill. 2009.

[8] L. Sepulchre, M. Fadel and M. Pietrzak-David, « Improvement of the digital control of a high speed PMSM for vehicle application, » *2016 Eleventh International Conference on Ecological Vehicles and Renewable Energies (EVER)*, Monte Carlo, 2016, pp. 1-9.

[9] L. Xu, Y. Zhang, et M. K. Guven, « A new method to optimize q-axis voltage for deep flux weakening control of IPM machines based on single current regulator », in *2008 International Conference on Electrical Machines and Systems*, 2008, p. 2750-2754.

[10] Y. Zhang, L. Xu, K. G. Mustafa, S. Chi, M. Illindala, et others, « Experimental verification of deep field weakening operation of a 50-kW IPM machine by using single current regulator », *IEEE Trans. Ind. Appl.*, vol. 47, nº 1, p. 128–133, 2011.

[11] Z. Lei, X. Shan, W. Xuhui, L. Yaohua, et K. Liang, « A new deep field-weakening strategy of IPM machines based on single current regulator and voltage angle control », in *2010 IEEE Energy Conversion Congress and Exposition*, 2010.

[12] Z. Lei, W. Xuhui, Z. Feng, K. Liang, et Z. Baocang, « Deep field-weakening control of PMSMs for both motion and generation operation », in *Electrical Machines and Systems (ICEMS), 2011 International Conference on*, 2011, p. 1–5.